

## Quenched bond randomness in marginal and non-marginal Ising spin models in 2D

To cite this article: N G Fytas *et al* *J. Stat. Mech.* (2008) P11009

View the [article online](#) for updates and enhancements.

### Related content

- [Wang–Landau study of the random bond square Ising model with nearest-andnext-nearest-neighbor interactions](#)  
N G Fytas, A Malakis and I Georgiou
- [First-order transition features of the 3D bimodal random-field Ising model](#)  
N G Fytas, A Malakis and K Eftaxias
- [Phase transition in the two-dimensional dipolar planar rotator model](#)  
L A S Mól and B V Costa

### Recent citations

- [Intrinsic convergence properties of entropic sampling algorithms](#)  
Rolando Elio Belardinelli *et al*
- [Corrections to scaling in the dynamic approach to the phase transition with quenched disorder](#)  
L. Wang *et al*
- [Wetting and interfacial adsorption in the Blume-Capel model on the square lattice](#)  
N. G. Fytas and W. Selke



**IOP | ebooks™**

Bringing together innovative digital publishing with leading authors from the global scientific community.

Start exploring the collection—download the first chapter of every title for free.

# Quenched bond randomness in marginal and non-marginal Ising spin models in 2D

**N G Fytas, A Malakis and I A Hadjiagapiou**

Department of Physics, Section of Solid State Physics, University of Athens,  
Panepistimiopolis, GR 15784 Zografos, Athens, Greece  
E-mail: [nfyas@phys.uoa.gr](mailto:nfyas@phys.uoa.gr), [amalakis@phys.uoa.gr](mailto:amalakis@phys.uoa.gr) and [ihatziag@phys.uoa.gr](mailto:ihatziag@phys.uoa.gr)

Received 22 September 2008

Accepted 17 October 2008

Published 11 November 2008

Online at [stacks.iop.org/JSTAT/2008/P11009](http://stacks.iop.org/JSTAT/2008/P11009)  
[doi:10.1088/1742-5468/2008/11/P11009](https://doi.org/10.1088/1742-5468/2008/11/P11009)

**Abstract.** We investigate and contrast, via entropic sampling based on the Wang–Landau algorithm, the effects of quenched bond randomness on the critical behavior of two Ising spin models in 2D. The random bond version of the superantiferromagnetic (SAF) square model with nearest- and next-nearest-neighbor competing interactions and the corresponding version of the simple Ising model are studied, and their general universality aspects are inspected by means of a detailed finite size scaling (FSS) analysis. We find that the random bond SAF model obeys weak universality, hyperscaling, and exhibits a strong saturating behavior of the specific heat due to the competing nature of interactions. On the other hand, for the random Ising model we encounter some difficulties as regards a definite discrimination between the two well-known scenarios of the logarithmic corrections versus the weak universality. However, a careful FSS analysis of our data favors the field theoretically predicted logarithmic corrections.

**Keywords:** classical Monte Carlo simulations, classical phase transitions (theory), finite-size scaling, disordered systems (theory)

---

## Contents

<b>1. Introduction</b>	<b>2</b>
<b>2. Simulation schemes and numerical details</b>	<b>3</b>
<b>3. The random bond square SAF model: competing interactions</b>	<b>6</b>
<b>4. The marginal case of the 2D random bond Ising model</b>	<b>11</b>
<b>5. Conclusions</b>	<b>14</b>
<b>Acknowledgments</b>	<b>15</b>
<b>References</b>	<b>15</b>

---

## 1. Introduction

The understanding of the role played by impurities in the nature of phase transitions is of great importance, both from experimental and theoretical perspectives. First-order phase transitions are known to be dramatically softened in the presence of quenched randomness [1]–[6], while continuous transitions may have their exponents altered for random fields or random bonds [3, 7, 8]. There are some very useful phenomenological arguments and some, perturbative in nature, theoretical results, pertaining to the occurrence and nature of phase transitions in the presence of quenched randomness [3], [9]–[13]. The most celebrated criterion is that suggested by Harris [7]. This criterion relates directly the persistence, for random bonds, of the non-random behavior to the specific heat exponent  $\alpha_p$  of the pure system. According to this criterion, if  $a_p$  is positive, then the disorder will be relevant, i.e., under the effect of the disorder, the system will reach a new critical behavior. Otherwise, if  $a_p$  is negative, disorder is irrelevant and the critical behavior will not change. The value  $\alpha_p = 0$  gives an inconclusive, marginal case. The 2D Ising model falls into this category; it is the most studied case, but is still controversial [14]. In general and despite the intensive efforts of the last few years on several different models, our current understanding of the quenched randomness effects is rather limited and the situation appears still unclear for both cases of first- and second-order phase transitions. The present paper aims to contribute to our knowledge of the effects of quenched bond disorder on second-order phase transitions. In this quite active field of research, resorting to large scale Monte Carlo simulations is often necessary and useful, and following this recipe, we applied some numerical schemes recently developed by our group—see reference [15] and references therein—to two types of random bond Ising models.

In the first part of the paper we present an extension of our numerical investigation of a random bond spin model in 2D with competing interactions, known as the random bond square SAF model [16]. Details of the pure and random version of this model with competing interactions and the motivation for such a study will be given below in the corresponding section, but can also be found in our recently published letter [16] and in other related papers in the literature [17]. Furthermore, in the second part of our work, in

a parallel study—using the same numerical techniques—we attempt to shed new light on the well-known random bond version of the 2D (simple) Ising model. Our investigation will be related to the extensive relevant literature concerning this case [18]–[58]. In particular, our discussion will focus on the main point of the last two decades, concerning two well-known conflicting scenarios, namely the logarithmic corrections [18, 19, 21, 22] versus the weak universality scenario [31, 32, 59, 60].

The rest of the paper is organized as follows. In section 2 we outline an extensive entropic sampling program. This program is based on (i) the Wang–Landau (WL) method [61], (ii) the dominant energy restriction scheme [62], and (iii) a second-stage improvement that combines the WL method [61] and some new ideas [15, 16, 63], suitable for the study also of disordered systems. Our FSS analysis of the numerical data and the corresponding discussion of the random bond versions of the square SAF model and the 2D Ising model are presented in sections 3 and 4, respectively. Finally, our conclusions are summarized in section 5.

## 2. Simulation schemes and numerical details

Importance sampling methods have been for many years the main tools in condensed matter physics and critical phenomena [64]–[68]. However, for complex systems, effective potentials may have a rugged landscape, that becomes more pronounced with increasing system size. In such cases, these traditional methods become inefficient, since they cannot overcome such barriers in the state space. A large number of generalized ensemble methods have been proposed to overcome such problems [61], [67]–[82]. One important class of these methods emphasizes the idea of directly sampling the energy density of states (DOS) and may be called the entropic sampling methods [67]. In entropic sampling, instead of sampling microstates with probability proportional to  $e^{-\beta E}$ , we sample microstates with probability proportional to  $[G(E)]^{-1}$ , where  $G(E)$  is the DOS, thus producing a flat energy histogram. The prerequisite for the implementation of the method is finding the DOS information of the system, a problem that can now be handled in many adequate ways via a number of interesting approaches proposed in the last two decades. The most remarkable examples are the Lee entropic [69, 70], the multicanonical [73, 74], the broad histogram [71], the transition matrix [72], the WL [61], and the optimal ensemble methods [82].

In particular, the WL algorithm [61] is one of the most refreshing variations of the Monte Carlo simulation methods introduced in the last years. The algorithm has already been successfully used in many problems of statistical physics, biophysics, and others [83]–[98]. To apply the WL algorithm, an appropriate energy range of interest has to be identified and a WL random walk is performed in this energy subspace. Trials from a spin state with energy  $E_i$  to a spin state with energy  $E_f$ , using local spin flip dynamics, are accepted according to the transition probability

$$p(E_i \rightarrow E_f) = \min \left[ \frac{G(E_i)}{G(E_f)}, 1 \right]. \quad (1)$$

During the WL process the DOS  $G(E)$  is modified ( $G(E) \rightarrow f * G(E)$ ) after each spin flip trial by a modification factor  $f > 1$ . In the WL process ( $j = 1, 2, \dots, j_f$ ) successive refinements of the DOS are achieved by decreasing the modification factor  $f_j$ .

Most implementations use an initial modification factor  $f_{j=1} = e \approx 2.71828\dots$ , a rule  $f_{j+1} = \sqrt{f_j}$ , and a 5%–10% flatness criterion (on the energy histogram) in order to move to the next refinement level ( $j \rightarrow j+1$ ) [61]. The process is terminated at a sufficiently high level ( $f \approx 1$ , whereas the detailed balanced condition limit is  $f \rightarrow 1$ ).

In the last few years, there have been several papers dealing with improvements and sophisticated implementations of the WL iterative process [63, 70, 84, 91, 97], [99]–[101]. The present authors have introduced a dominant energy subspace implementation of the above entropic methods, called the critical minimum energy subspace (CrMES) method [62]. This is a method of a systematic restriction of the energy space, with increasing lattice size, by which one can determine all finite size thermal anomalies of the system from the final accurate DOS, and also other (magnetic) anomalies of the system, by accumulating appropriate histogram data in the final almost entropic stage of the process. The (WL) random walk takes place in a restricted energy subspace ( $E_1, E_2$ ) and this practice produces an immense speed-up, without introducing observable errors. It has been shown that the method can be followed successfully in pure systems undergoing second- or first-order phase transitions [62, 85] and also in more complex systems with complicated free energy landscapes, such as the 3D random field Ising model [15].

For the simulation of the random bond models considered in this paper, we followed the general framework of the implementation of the above described scheme. In particular, we followed most of the details of the implementation applied recently to the 3D random field Ising model and outlined for the random bond version of the SAF model in our recently published letter [16]. In these papers, a two-stage strategy has been followed. In the first stage, a multi-range (multi-R) WL method was applied, where the total energy range was split into many subintervals [61] and the DOSs of these separate pieces were then joined at the end of the process. The WL refinement levels used in this first multi-R WL stage ( $j = 1, \dots, j_i$ ), were as follows:  $j_i = 18$  for  $L < 80$ ,  $j_i = 19$  for  $80 \leq L < 120$ , and  $j_i = 20$  for  $L \geq 120$ . In the second stage of the simulation (WL refinement levels:  $j = j_i - j_f$ ), a more demanding multi-R—but with larger energy pieces—or a one-range (one-R) approach was carried out. The identification of the appropriate energy subspace ( $E_1, E_2$ ) for the entropic sampling of each disorder realization was carried out by applying our CrMES restriction [62] and taking the union subspace at both pseudocritical temperatures of the specific heat and susceptibility. This union subspace, extended by 10% from each side, the low energy and high energy sides, is in most cases sufficient for an accurate estimation of all finite size anomalies. The identification of the appropriate energy subspace was carried out in the first multi-R WL stage, using originally a very wide energy subspace. After the first identification, the same first-stage process ( $j = 1, \dots, j_i$ ) was repeated several times, typically  $\sim 4$ – $6$  times, in the new restricted energy subspace. In our experience, this repeated application of this first-stage multi-R WL approach greatly improves accuracy, and then the resulting accurate DOS is used again for a final and more accurate redefinition of the subspace ( $E_1, E_2$ ), in which the final entropic scheme (second stage) is applied. Thus, the final entropic WL stage ( $j = j_i - j_f$ ), where  $j_f = j_i + 4$  in all cases, was carried out in this accurately defined subspace in a one-R or in a multi-R approach. For the present models, it was found that a final multi-R approach with large subranges (see below) is in fact sufficiently accurate. Therefore, since the multi-R approach of the original WL scheme improves efficiency, we applied, for most of our simulations, this multi-R WL approach also in the final entropic stage, using energy

subintervals three times larger than in the initial multi-R stage. The energy subintervals of the first stage were chosen to correspond to rather large subspaces, with their sizes depending on the disorder strength. Taking the pure system as reference, these energy subintervals could be chosen of the order of 50–100 energy levels, depending on the lattice size. In the disorder case, the subinterval sizes are multiplied by the factor induced due to the new multiplicity of energy levels, giving for instance a factor 4 for the disorder strength  $r = 3/5 = 0.6$ , where  $r$  is the ratio of weak over strong bond interactions (see also section 3).

As pointed out above, the need for using in the final stage the described multi-R approach, instead of a one-R approach, is a consequence of the slow convergence at the high WL levels. It is possible to overcome this slow convergence by using a looser flatness criterion or an alternative Lee entropic final stage, as proposed in [70] and applied by the present authors [15]. However, recently a different alternative has been proposed by Belardinelli and Pereyra (BP) [63], which is free of the application of the energy-histogram flatness criterion. Following their proposal, one is using, in the final stage, an almost continuously changing modification factor adjusted according to the rule  $\ln f \sim t^{-1}$ . Since  $t$  is the Monte Carlo time, using a time step conveniently defined proportional to the size of the energy subinterval, the efficiency of this scheme is independent of the size of the subintervals and therefore the method provides the same efficiency in both multi-R and one-R approaches. Furthermore, from the tests performed by these authors, and also from our comparative studies in the 2D pure Ising model (unpublished), the error behavior of this method seems superior to the original WL process, lessening to some extent the saturation-error problem of the WL method. Accordingly, we have also applied this alternative route for the final stage of our simulations using a one-R approach. In particular, the disorder strength case  $r = 9/11 = 0.818$  of the random bond square SAF model, and all simulations corresponding to the larger sizes  $L = 160$  and  $200$  of the random bond Ising model, were addressed using this alternative. From our comparative tests, we found that both approaches (the BP and the multi-R WL approach) produced very accurate results, with the BP approach giving superior estimates for the pseudocritical temperatures of the models.

Both disordered models were simulated for two values of the disorder strength  $r$ . For the random bond square SAF model we chose the values  $r = 9/11 = 0.818$  and  $r = 3/5 = 0.6$ , whereas for the random bond Ising model the values  $r = 3/5 = 0.6$  and  $r = 1/7 = 0.142$  have been considered. Square lattices, using periodic boundary conditions, with linear sizes  $L$  in the range  $L = 20$ – $120$  or  $L = 20$ – $200$  (disorder strength case  $r = 1/7 = 0.142$ ) were used. A total of 200 disorder realizations were generated and simulated for each disorder case and lattice size. Even for the larger lattice sizes the statistical errors of the WL method (WL errors), used for the estimation of thermal and magnetic properties of a particular realization, were found to be much smaller than the statistical errors of the disorder averaging, this arising from the fact that we have used a finite number, 200, of disorder realizations. Therefore, the WL errors are not shown in our graphs, whereas the latter errors of finite disorder sampling are presented in our figures as error bars. The mean values over disorder will be denoted as  $[\dots]_{\text{av}}$ , the corresponding maxima as  $[\dots]_{\text{av}}^*$ , and finally the individual maxima as  $[\dots]^*_{\text{av}}$ . Since in the fitting attempts of the following sections, we have used mainly data from the peaks of the disorder averaged curves (i.e.  $[C]_{\text{av}}^*$ ), their finite disorder sampling errors are the relevant statistical



errors to use in the fitting attempts. These errors have been estimated by two similar methods, using groups of 25–50 realizations for each lattice size and the jackknife method or a straightforward variance calculation (blocking method) [67]. The jackknife method yielded some reasonably conservative errors, about 10–20% larger than the corresponding calculated standard deviations, and are shown as error bars in our figures. Finally, let us point out that in all cases studied, the sample-to-sample fluctuations for the individual maxima are much larger than the corresponding finite disorder sampling errors.

### 3. The random bond square SAF model: competing interactions

In this section we extend our investigation to the effects of quenched bond randomness on the square Ising model with nearest-neighbor ( $J_{nn}$ ) and next-nearest-neighbor ( $J_{nnn}$ ) antiferromagnetic interactions. In zero field, the pure square SAF model is governed by the Hamiltonian

$$\mathcal{H}_p = J_{nn} \sum_{\langle i,j \rangle} S_i S_j + J_{nnn} \sum_{(i,j)} S_i S_j, \quad (2)$$

where here both nearest-neighbor ( $J_{nn}$ ) and next-nearest-neighbor ( $J_{nnn}$ ) interactions are assumed to be positive. It is well known that the model develops at low temperatures SAF order for  $R = J_{nn}/J_{nnn} > 0.5$  [102]–[104] and by symmetry the critical behavior associated with the SAF ordering is the same for  $J_{nn} \rightarrow -J_{nn}$ . For the case  $R = 1$ , that we deal with, the pure system undergoes a second-order phase transition, in accordance with the commonly accepted scenario for many years of a non-universal critical behavior with exponents depending on the coupling ratio  $R$  [102, 103], [105]–[107]. The recent numerical study of Malakis *et al* [108] has refined earlier estimates [103, 106] for the correlation length exponent  $\nu$  and values very close to those for the 2D three-state Potts model  $\nu_p$  (Potts) = 5/6 [109] were obtained. From the FSS of the pseudocritical temperatures [108] it was found that  $\nu_p$  (SAF;  $R = 1$ ) = 0.8330(30) and the subsequent study of Monroe and Kim [110], using the Fisher zeros of the partition function, yielded a quite closely matching estimate:  $\nu_p$  (SAF;  $R = 1$ ) = 0.848(1). Furthermore, from the FSS of the specific heat data an estimate for the ratio  $\alpha_p/\nu_p = 0.412(5)$  was also found [108]. Finally, from the magnetic data and in accordance with an earlier conjecture of Binder and Landau [103], Malakis *et al* [108] found additional evidence of the weak universality scenario [59, 60] and obtained the values  $\beta_p/\nu_p = 0.125$  and  $\gamma_p/\nu_p = 1.75$ . The values of the above three ratios of exponents satisfy the Rushbrooke relation, assuming that  $\nu_p = 0.8292$ , which is very close to the estimate obtained from the shift behavior of the SAF  $R = 1$  model, thus providing self-consistency to the estimation scheme. From these results, it is tempting to conjecture, as was pointed out in [16], that the SAF model with  $R = 1$  has the same thermal exponents as the 2D three-state Potts model ( $\nu_p = 5/6 = 0.833\cdots$  and  $\alpha_p = 1/3 = 0.333\cdots$  [109]), but the respective values of the magnetic critical exponents are different ( $\beta_p/\nu_p = 2/15 = 0.133\cdots$  and  $\gamma_p/\nu_p = 26/15 = 1.733\cdots$  for the 2D three-state Potts model [109]).

Considering now the random bond distribution [16]

$$P(J_{ij}) = \frac{1}{2}[\delta(J_{ij} - J_1) + \delta(J_{ij} - J_2)]; \quad \frac{J_1 + J_2}{2} = 1; \quad r = \frac{J_2}{J_1}, \quad (3)$$

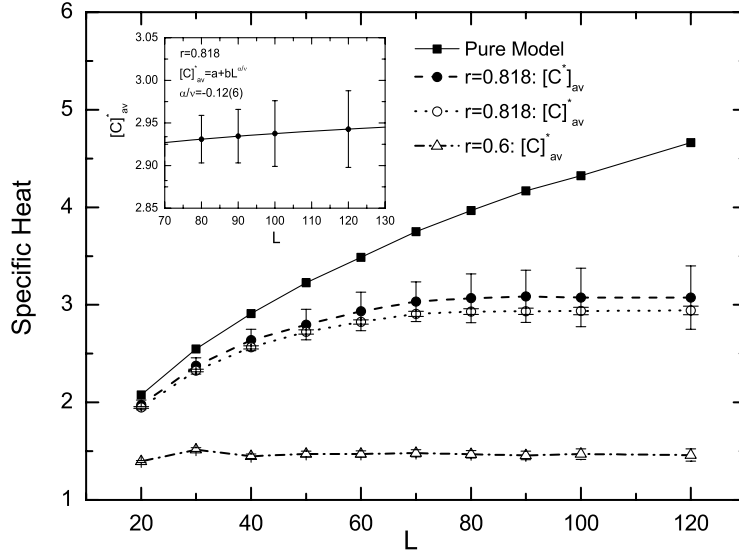


**Figure 1.** Size dependence of the maxima of the specific heat for the pure (filled squares; data taken from [108]) and the random bond (filled and open circles for  $r = 0.818$  and open triangles for  $r = 0.6$ ) square SAF model. The inset shows a power law fit for the case  $r = 0.818$  for  $L \geq 80$  giving a negative value for the exponent  $\alpha/\nu$  of the order of  $-0.12(6)$ .

where the ratio  $r$  stands for the disorder strength, the Hamiltonian of equation (1) is transformed into the following disordered one:

$$\mathcal{H} = \sum_{\langle i,j \rangle} J_{ij} S_i S_j + \sum_{(i,j)} J_{ij} S_i S_j. \quad (4)$$

The critical behavior of the above defined random model for the case  $r = 3/5 = 0.6$  has been outlined in reference [16], where apart from the verification of the weak universality scenario, a strong saturating behavior of the specific heat has been witnessed. Here, we extend our study to a weaker disorder strength, namely the case  $r = 9/11 = 0.818$ .

Let us start the presentation of our results with the most striking effect of the bond randomness on the specific heat of the square SAF model. In figure 1 we contrast the size dependence of the specific heat maxima of the pure (filled squares) and the random bond model (filled and open circles for  $r = 0.818$  and open triangles for the case  $r = 0.6$ ). For the case  $r = 0.818$  we show two data set points for the specific heat, corresponding to the two averaging processes discussed previously in section 2. Note that the error bars for the quantity  $[C^*]_{av}$  shown reflect the sample-to-sample fluctuations, whereas all other error bars are statistical errors due to the finite number of disorder realizations (jackknife errors discussed in section 2). The suppression of the specific heat maxima is clear for both disorder strength values and of course it is much stronger for the case  $r = 0.6$ , for which a clear saturation is observed even for the smaller sizes shown ( $L = 40$ ). For the present value  $r = 0.818$  we show in the inset of figure 1 a power law fitting attempt of the form  $[C]_{av}^* \sim C_\infty + bL^{\alpha/\nu}$  for sizes  $L \geq 80$  which gives a negative value for the exponent  $\alpha/\nu$  of the order of  $-0.12(6)$ . Notably, this value of  $\alpha/\nu$  will be shown to be compatible with the one obtained by an alternative method via the Rushbrook relation.



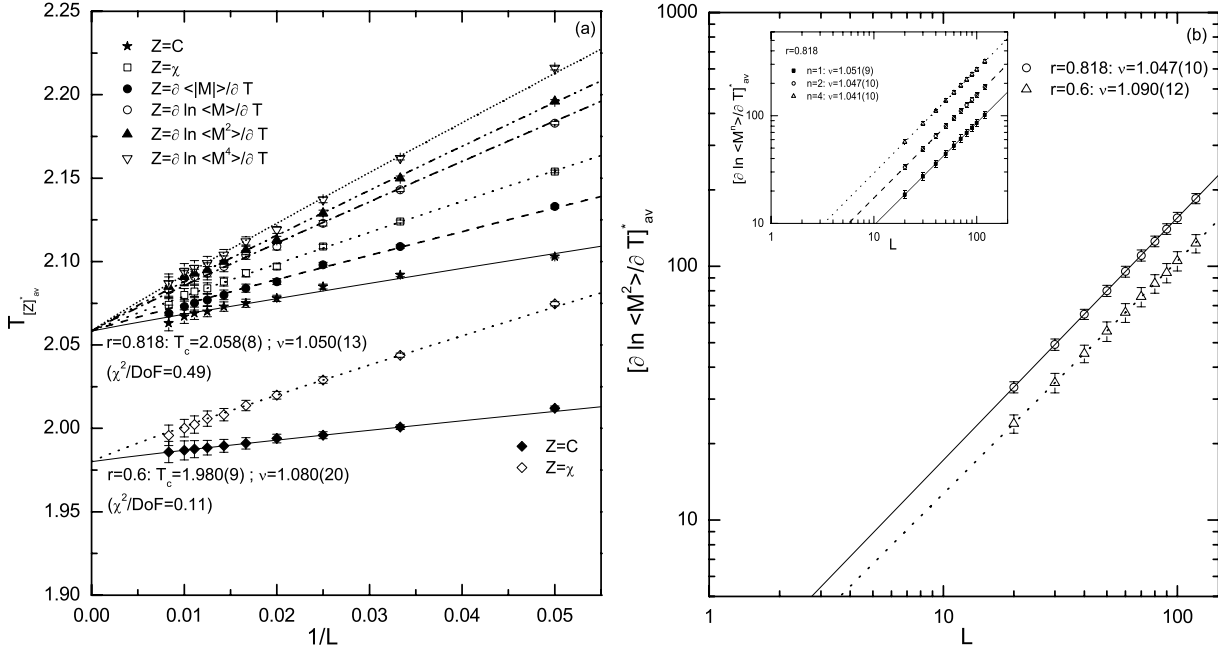


**Figure 2.** (a) Simultaneous fittings of several pseudocritical temperatures of the random bond square SAF model for the two values of  $r$  considered:  $r = 0.818$  and  $0.6$ . (b) Log-log plot of the maxima of the average second-order logarithmic derivative of the order parameter of the random bond square SAF model also for  $r = 0.818$  and  $0.6$ . The inset shows a log-log plot of the maxima of the average logarithmic derivatives of the order parameter of first, second, and fourth order, for the case  $r = 0.818$ . Linear fits are applied for  $L \geq 30$ .

In figure 2(a) we present the FSS behavior of several pseudocritical temperatures of the model  $T_{[Z]_{av}}^*$ , i.e. the temperatures corresponding to the maxima of several average curves, such as the specific heat ( $Z = C$ ), the magnetic susceptibility ( $Z = \chi$ ), the absolute order parameter derivative with respect to the temperature ( $Z = \partial \langle |M| \rangle / \partial T$ ), and the logarithmic derivatives of several powers of the order parameter with respect to the temperature ( $Z = \partial \ln \langle M^n \rangle / \partial T$ ,  $n = 1, 2$  and  $4$ ). For the case  $r = 0.818$  all of the above mentioned six pseudocritical temperatures are presented and are compared to the case  $r = 0.6$  [16]. The lines show two sets of simultaneous fitting attempts, according to the shift relation

$$T_{[Z]_{av}}^* = T_c + bL^{-1/\nu}, \quad (5)$$

giving  $T_c = 2.058(8)$  for  $r = 0.818$  and  $T_c = 1.980(9)$  for  $r = 0.6$ , for the critical temperature of the disordered model. Note that the corresponding critical temperature of the pure system is  $T_{c,p} = 2.0823(17)$  [108]. The values for  $\chi^2/\text{DoF}$  for the fits shown depend on the method used to evaluate the statistical errors (jackknife or simple standard deviation errors) and in all cases studied in this paper vary in the range  $0.1$ – $0.5$ . A first estimation of the critical exponent  $\nu$  of the correlation length is obtained from the above shift behavior and is  $\nu = 1.050(13)$  and  $\nu = 1.080(20)$  for  $r = 0.818$  and  $0.6$  respectively, as illustrated in the graph. An alternative estimation of the exponent  $\nu$  is attempted now

from the FSS analysis of the logarithmic derivatives of the order parameter<sup>1</sup> with respect to the temperature [4, 111]

$$\frac{\partial \ln \langle M^n \rangle}{\partial T} = \frac{\langle M^n E \rangle}{\langle M^n \rangle} - \langle E \rangle, \quad (6)$$

which scale as  $L^{1/\nu}$  with the system size. In figure 2(b) we consider on a log-log scale the size dependence of the maxima of the average second-order logarithmic derivative of the order parameter for  $r = 0.818$  (open circles) and  $r = 0.6$  (open triangles). The solid and dotted lines are corresponding linear fits whose slopes provide respectively estimates for  $1/\nu$  and, thus, for the exponent  $\nu$ . It is clear for the figure that the slopes of the lines are different and the results that we obtain from the linear fits are  $\nu = 1.047(10)$  and  $\nu = 1.090(12)$  for  $r = 0.818$  and  $0.6$ , respectively. In the corresponding inset of figure 2(b) we present the first-order (filled squares), second-order (open circles), and fourth-order (open triangles) maxima of the average over the ensemble of realizations logarithmic derivatives of the order parameter for the case  $r = 0.818$ . The solid, dashed, and dotted lines shown are corresponding linear fits whose slopes provide an average estimate for the exponent  $\nu$  of the order of  $\nu = 1.046(10)$ . These results for the exponent  $\nu$  for both values of the disorder strength  $r$  compare favorably with the estimate of  $\nu$  from the above shift behavior shown in panel (a) of figure 2. Thus, in comparison with its value of the pure model, the exponent  $\nu$  for the disordered model shows an increase of the order of 20% for the case  $r = 0.818$  and 30% for the case  $r = 0.6$ , reflecting, in both cases, the strong influence of the disorder on the thermal properties of the system. It is noteworthy that our estimates for the exponent  $\nu$  are in agreement with the inequality  $\nu \geq 2/D$  derived by Chayes *et al* [8] for disordered systems.

Turning now to the magnetic properties of the model, we present in figure 3(a) on a log-log scale the FSS behavior of the average order parameter for  $r = 0.818$  (open circles) at  $T_c = 2.058$  and for  $r = 0.6$  (open triangles) at  $T_c = 1.98$ . The straight lines show linear fits for  $L \geq 30$  with a slope of  $0.124(6)$  for  $r = 0.818$  and  $0.126(5)$  for  $r = 0.6$ . Thus, these two estimates for the ratio  $\beta/\nu$  indicate that although the exponent  $\beta$  increases with disorder, the ratio  $\beta/\nu$  remains unchanged from its pure value, i.e.  $\beta/\nu = \beta_p/\nu_p = 0.125$  [16, 108]. Correspondingly, we show in panel (b) of figure 3 the behavior of the magnetic susceptibility that provides estimates for the ratio  $\gamma/\nu$ . The open circles refer to the case  $r = 0.818$  and the open triangles to the case  $r = 0.6$ . The solid and dotted lines are linear fits giving the values  $\gamma/\nu = 1.749(9)$  and  $\gamma/\nu = 1.751(10)$ , respectively. Thus, the ratio  $\gamma/\nu$  maintains the value of the pure model for both disorder strength values considered. The ratios  $\beta/\nu$  and  $\gamma/\nu$  for the disordered square SAF model appear to be the same as the corresponding ratios of the pure square SAF model but different from those of the 2D three-state Potts model. Therefore, our results reinforce both the weak universality scenario for the pure SAF model, as first predicted by Binder and Landau [103], and the generalized statement of weak universality in the presence of bond randomness, given by Kim [112] and concerning also the 2D random bond three-state Potts ferromagnet.

Finally, having estimated the ratios  $\beta/\nu$ ,  $\gamma/\nu$ , and the exponent  $\nu$ , we attempt to estimate the specific heat exponent  $\alpha$  using either the Rushbrook ( $\alpha + 2\beta + \gamma = 2$ )

<sup>1</sup> For the definition of the order parameter we follow [108], using the four sublattice magnetizations:  $M = \sum_{i=1}^4 |M_i|/4$ .

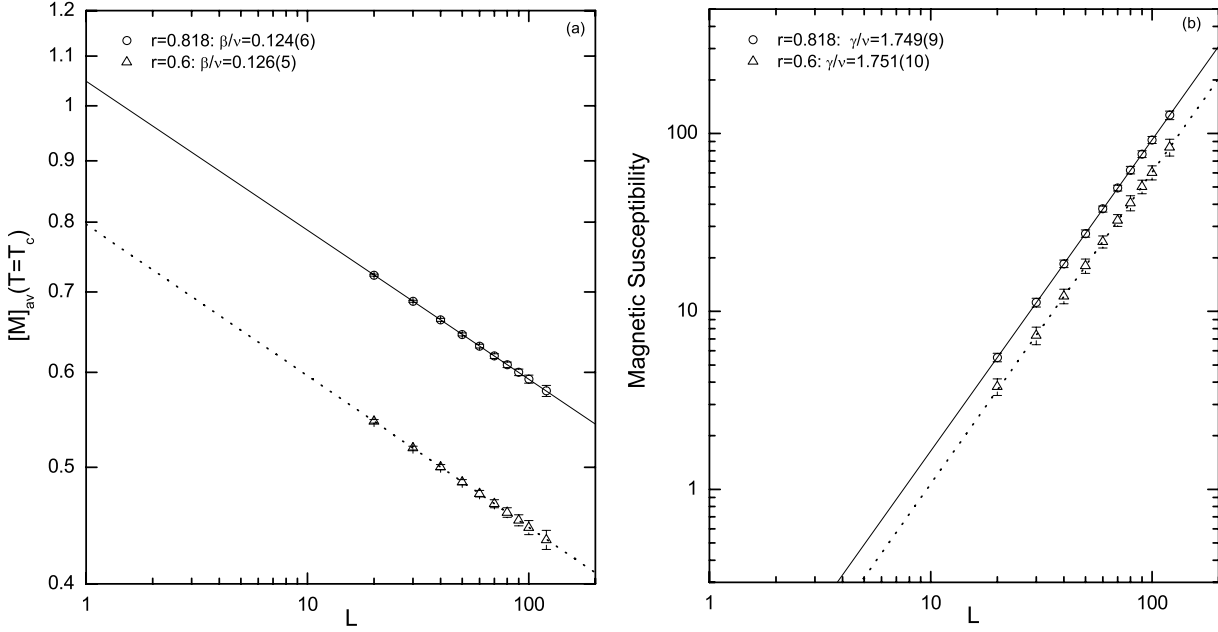


**Figure 3.** (a) Log-log plot of the size dependence of the average magnetization of the random bond square SAF model at the estimated corresponding critical temperatures for  $r = 0.818$  and  $0.6$ . (b) Log-log plot of the size dependence of the maxima of the average magnetic susceptibility of the random bond square SAF model for  $r = 0.818$  and  $0.6$ . In both panels, the solid and dotted lines are corresponding linear fits for  $L \geq 30$ .

or equivalently, since  $2\beta/\nu + \gamma/\nu = 2$ , the hyperscaling ( $2 - \alpha = D\nu$ ) relation. For the case  $r = 0.818$  we find a value  $\alpha/\nu = -0.09(4)$  which is in agreement with the value  $\alpha/\nu = -0.12(6)$  estimated from the fitting of the larger specific heat data shown in the inset of figure 1. In the case of a non-divergent specific heat it is quite interesting to consider also, rather than the specific heat, the internal energy scaling at the estimated critical temperature. This provides an estimate for the exponent ratio  $(\alpha - 1)/\nu$ , which may be more precise [113]. We finally carried out such a fitting using the larger sizes ( $L \geq 80$ ) for the values of the critical energy (at  $T_c = 2.058$ ) and we found  $(\alpha - 1)/\nu = -1.04(4)$ . This result, when combined with the estimate for  $\nu$  from the shift behavior ( $\nu = 1.050(13)$ ) gives a value  $\alpha/\nu = -0.09(3)$ , an intriguing coincidence, in full agreement with the above value obtained for this ratio, via the Rushbrook relation. For the case  $r = 0.6$  [16], the saturation effect is much more stronger and an even more negative value for the specific heat exponent  $\alpha$  is obtained:  $\alpha = -0.17(4)$ . From the above and in agreement with our preliminary observation in [16], it turns out that this strong saturating behavior of the specific heat is completely different from the behavior of the 2D random bond three-state Potts ferromagnet [112, 114]. There, a specific heat diverging behavior is obtained for disorder strengths  $r = 0.9, 0.5$ , and  $0.25$  [112] and an increasing but progressively saturating behavior is obtained only for the very strong disorder  $r = 0.1$  [114]. This behavior of the specific heat of the random bond square SAF model may presumably be attributed to the competitive nature of interactions, responsible for the observed sensitivity of the SAF model to bond randomness.

#### 4. The marginal case of the 2D random bond Ising model

The Hamiltonian of the random bond version of the 2D Ising model system is given by

$$\mathcal{H} = - \sum_{\langle i,j \rangle} J_{ij} S_i S_j, \quad (7)$$

where again the implementation of the bond disorder follows the binary distribution (3) of ferromagnetic interaction strengths. With this distribution the random Ising system exhibits a unique advantage: that its critical temperature  $T_c$  is exactly known [115, 116] as a function of the disorder strength  $r$  through

$$\sinh(2J_1/T_c) \sinh(2rJ_1/T_c) = 1, \quad (8)$$

where  $r = J_2/J_1$  and  $k_B = 1$ . This gives the opportunity of carrying out the FSS analysis at the exact  $T_c(r)$ , a practice that greatly reduces statistical errors. Furthermore, one may check for accuracy this numerical scheme by comparing the estimated critical temperature (via the shift behavior) with the exact result, as we have also done here.

At this point, it is useful to briefly discuss the two main and mutually excluded scenarios [14] mentioned in section 1. The logarithmic corrections scenario is based on the quantum field theory results of Dotsenko and Dotsenko [18], and of Shalaev [19], Shankar [21], and Ludwig [22]. According to this scenario—supported theoretically for the case of weak disorder—the presence of quenched disorder changes the critical properties of the system only through a set of logarithmic corrections to the pure system behavior. The specific heat  $C$  is expected to diverge on approach to the critical temperature  $T_c$  in a double-logarithmic form:  $C \propto \ln(\ln t)$ , where  $t = |T - T_c|/T_c$  is the reduced critical temperature. On the other hand, according to the weak universality scenario [31, 32, 59, 60], critical quantities, such as the zero-field susceptibility, magnetization, and correlation length, display power law singularities, with the corresponding exponents  $\gamma$ ,  $\beta$ , and  $\nu$  changing continuously with the disorder strength; however this variation is such that the ratios  $\gamma/\nu$  and  $\beta/\nu$  remain constant at the pure system's value. The specific heat of the disordered system is, in this case, expected to saturate [31].

Two significantly different values of the disorder strength, namely the cases  $r = 3/5 = 0.6$  and  $r = 1/7 = 0.142$ , have been investigated using our numerical scheme and our data will be presented and analyzed below. Due to marginality, the case  $r = 0.6$ , that produced in the SAF model a 5% temperature decline, gives here, through equation (8) a critical temperature  $T_c(r = 0.6) = 2.224\,19\dots$ , very close (2%) to the corresponding critical temperature of the pure system ( $T_{c;p} = 2.269\,18\dots$ ). Thus, we may call the first case ( $r = 3/5 = 0.6$ ) a weak disorder case and the second case ( $r = 1/7 = 0.142$ ) a strong disorder case, actually producing a significant temperature decline  $T_c(r = 0.142) = 1.779\,10\dots$ . Our simulations are extended to lattice sizes in the range  $L = 20\text{--}120$  for the weak disorder and in the range  $L = 20\text{--}200$  for the strong disorder, in the hope that we will observe the true asymptotic behavior of the model. For the calculation of the statistical errors due to the finite number of simulated realizations, we have followed again the practice outlined in section 2. The values of  $\chi^2/\text{DoF}$  for all the fits shown below are again in the range 0.1–0.5.

We start the presentation of our results with the case  $r = 3/5 = 0.6$  and our fitting attempts are summarized in figure 4. Figure 4(a) shows a simultaneous fitting—including

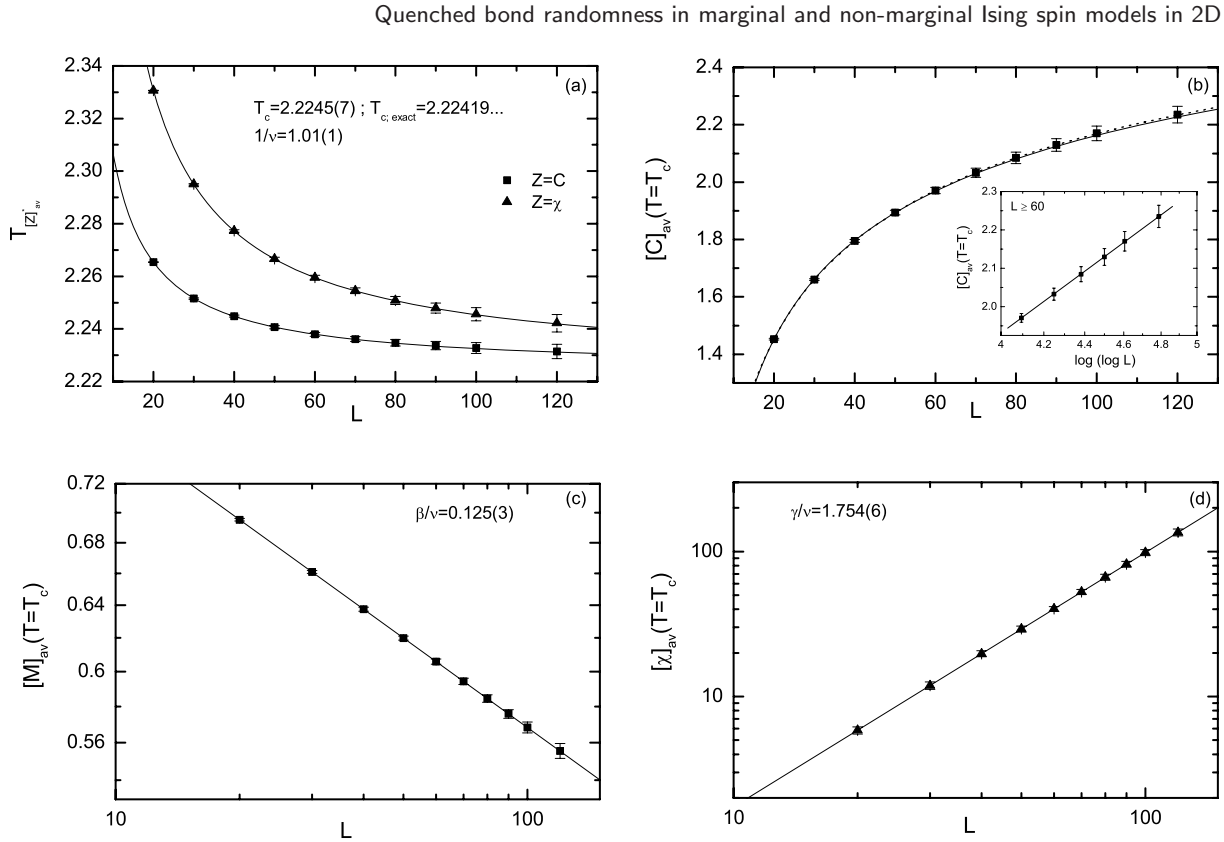


**Figure 4.** Critical behavior of the 2D random bond Ising model for  $r = 3/5 = 0.6$ . (a) Simultaneous fitting of two pseudocritical temperatures defined in the text and estimation of the correlation length exponent. (b) FSS behavior of the averaged specific heat at  $T_c(r = 0.6)$ . The solid and dotted lines are corresponding double-logarithmic and power law fits (see equations (9) and (10) in the text). The inset shows the specific heat data as a function of the double logarithm of the lattice size. A linear fit for  $L \geq 60$  is applied. (c) Log-log plot of the averaged magnetization at  $T_c(r = 0.6)$ . (d) Log-log plot of the averaged magnetic susceptibility at  $T_c(r = 0.6)$ . In both panels (c) and (d) a linear fit is applied. Note that all fitting attempts shown have been performed for  $L \geq 20$ .

all data points—using the shift behavior (5) for the estimation of the critical temperature and the correlation length exponent. Now, we have used the pseudocritical temperatures  $T_{[Z]_{av}}^*$  of the specific heat ( $Z = C$ ) and magnetic susceptibility ( $Z = \chi$ ). As shown in the panel, the estimated value for the critical temperature is  $T_c = 2.2245(7)$ , in excellent agreement with the exact value. Correspondingly, the estimate of the inverse of the correlation length exponent is  $1/\nu = 1.01(1)$ , which provides a value for  $\nu$  of the order  $\nu = 0.99(1)$ , very close to the value  $\nu = 1$  for the pure model.

In panel (b) of figure 4 we illustrate the data for the averaged specific heat at the exact critical temperature. The solid and dotted lines are corresponding fits of the form

$$[C]_{av}(T = T_c) \sim C_1 + C_2 \ln(\ln L) \quad (9)$$

and

$$[C]_{av}(T = T_c) \sim C_\infty + bL^{\alpha/\nu}. \quad (10)$$

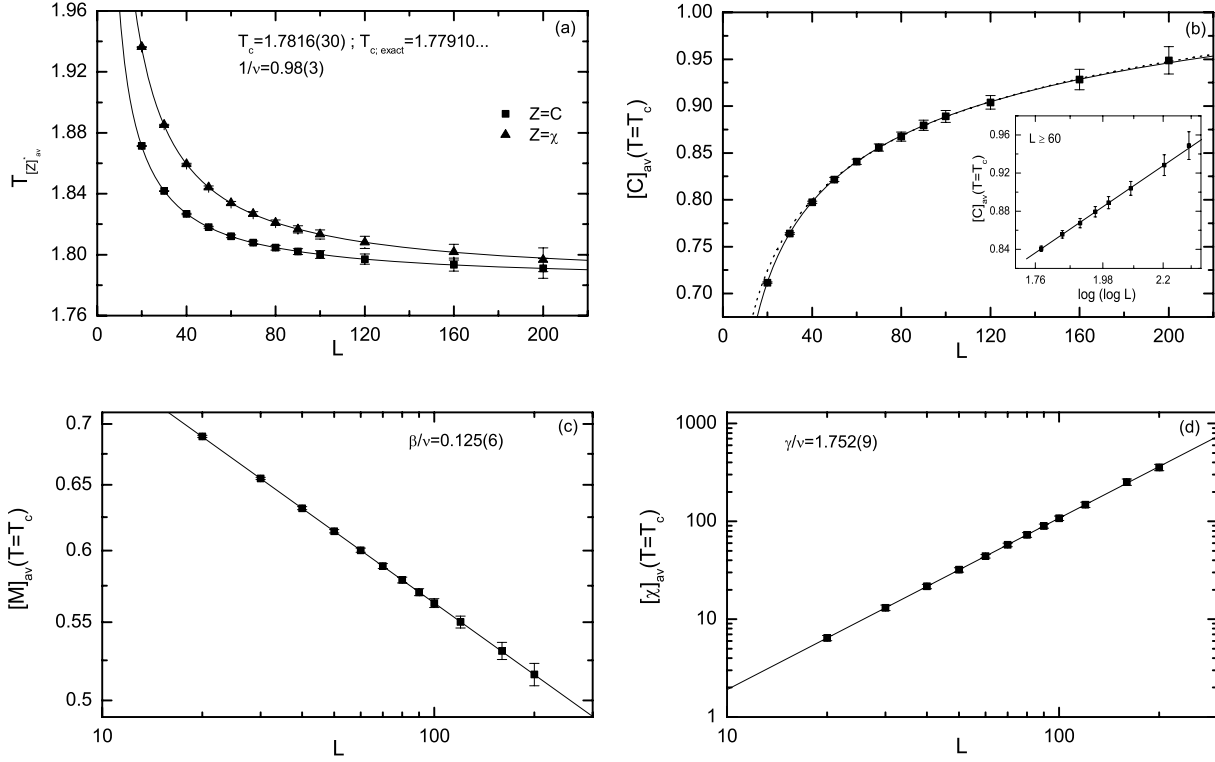


**Figure 5.** The same as figure 4 but for  $r = 1/7 = 0.142$ . Now data for lattice sizes up to  $L = 200$  are presented. All fitting attempts shown are performed for  $L \geq 60$ .

As is clear from this graph, one may not easily distinguish between the two lines, although a more careful analysis indicates that the double-logarithmic function is more stable. We have performed both kinds of fits for three sets of data points  $L_{\min} - L_{\max}$ . We fixed  $L_{\max} = 120$  and varied  $L_{\min}$  as follows:  $L_{\min} = 20$ ,  $L_{\min} = 50$ , and  $L_{\min} = 80$ . We have observed that although the values of  $\chi^2/\text{DoF}$  are comparable for the two functions (9) and (10), the coefficient  $C_2$  of equation (9) seems to be stable ( $C_2 \simeq 1.67(3)$ ), whereas the exponent  $\alpha/\nu$  of equation (10) fluctuates, with increasing  $L_{\min}$ , in the range  $-0.3$  to  $-0.2$ :  $(\alpha/\nu)(L_{\min} = 20) = -0.24(2)$ ,  $(\alpha/\nu)(L_{\min} = 50) = -0.21(4)$ , and  $(\alpha/\nu)(L_{\min} = 80) = -0.30(3)$ . Although for this case we cannot conclusively discriminate between the two alternatives, the inset in panel (b) shows that the specific heat data fit well to the double logarithm for lattice sizes  $L \geq 60$ . Finally, in panels (c) and (d) we plot the average magnetization and the average magnetic susceptibility at the critical temperature, respectively, as a function of the lattice size  $L$  in a log-log scale. In both cases a linear fit is applied for  $L \geq 20$  giving the values  $\beta/\nu = 0.125(3)$  and  $\gamma/\nu = 1.754(6)$ , i.e. the ratios of the magnetic exponents  $\beta/\nu$  and  $\gamma/\nu$  maintain the values  $\beta_p/\nu_p = 0.125$  and  $\gamma_p/\nu_p = 1.75$  of the pure model.

We proceed to present our results for the strong disorder strength  $r = 1/7 = 0.142$ . As was already stated above, for this value of  $r$  we have extended our simulations up to sizes  $L = 200$ . Figure 5 summarizes now the critical behavior for the case  $r = 0.142$  and, in particular, in figure 5(a) we estimate, via a simultaneous fitting attempt for the



larger lattices ( $L \geq 60$ ), the critical temperature and the correlation length exponent. The estimated value for the critical temperature is  $T_c = 1.7816(30)$ , in good agreement with the exact value. The production of the above accurate estimates for the critical temperatures, even in this strong disorder case, constitutes a concrete reliability test, in favor of the accuracy of our numerical scheme. The estimation of the inverse of the correlation length exponent is  $1/\nu = 0.98(3)$ , providing a value for  $\nu$  of the order  $\nu = 1.02(3)$ , which within error bars agrees with the pure model's correlation length exponent value. In panel (b) of figure 5 we plot the data for the averaged specific heat at the exact critical temperature. Again, the solid and dotted lines are corresponding fits of the forms (9) and (10) for the larger sizes ( $L \geq 60$ ). Our analysis for the quality of the fits for the three sets of data points  $L_{\min} - L_{\max}$ , with  $L_{\max} = 200$  and  $L_{\min} = 20, 50$ , and  $80$ , indicated a good trend for the values of  $\chi^2/\text{DoF}$  for the double-logarithmic fits (9) in the range  $0.1-0.3$ . Further reliability in favor of the logarithmic corrections scenario is provided by the stability of the coefficient  $C_2$ :  $C_2(L_{\min} = 20) = 0.412(4)$ ,  $C_2(L_{\min} = 50) = 0.410(6)$ ,  $C_2(L_{\min} = 80) = 0.418(7)$ , whereas the value of the exponent  $\alpha/\nu$  of the power law (10) approaches zero with increasing  $L_{\min}$ :  $(\alpha/\nu)(L_{\min} = 20) = -0.27(4)$ ,  $(\alpha/\nu)(L_{\min} = 50) = -0.20(6)$ , and  $(\alpha/\nu)(L_{\min} = 80) = -0.02(3)$ . From the above, we may conclude that our numerical data are more properly described, at least for the larger lattice sizes studied, by the double-logarithmic form (9). The inset in panel (b) of figure 5 shows again the specific heat data as a function of the double logarithm of the lattice size for  $L \geq 60$ . The solid line shown is an excellent linear fit. It should be noted that the above power law behavior ( $\alpha/\nu \rightarrow 0_-$ ) is in full agreement with the earlier observation of Wang *et al* [25] in the strong disorder regime ( $r = 1/4$  and  $1/10$ ) [25]. Note also that analogous results have been presented in figure 2 of [39] for the site diluted Ising model, where sizes up to  $L = 256$  have been considered. Finally, in panels (c) and (d) we plot the average magnetization and the average magnetic susceptibility at the critical temperature respectively, as a function of the lattice size  $L$  in a log-log scale. In both cases, the solid lines shown are linear fits for  $L \geq 60$  giving again within error bars the values of the pure model,  $\beta/\nu = 0.125(6)$  and  $\gamma/\nu = 1.752(9)$ , respectively.

Summarizing, we may point out that the difficulties observed in the case of weak disorder in discriminating between the two scenarios have been overcome by considering the strong disorder case and larger lattice sizes. In particular, we take as evidence in favor of the picture that emerged from the theoretical work of Dotsenko and Dotsenko [18], and the improved versions of Shalaev [19], Shankar [21], and Ludwig [22], the stability of our fitting attempts using the double-logarithmic law. Similar conclusions have also been reported from the extensive Monte Carlo studies of Wang *et al* [25] for the random bond model and also of Selke *et al* [43], Ballesteros *et al* [39], and Tomita and Okabe [48] for the site diluted model, from the transfer matrix approach of Araújo Reis *et al* [36, 40] for the random bond case, and, very recently, from the work of Kenna and Ruiz-Lorenzo [58] via an alternative approach that involves the density of Lee-Yang zeros of the site diluted model.

## 5. Conclusions

The effects induced by the presence of quenched bond randomness on the critical behavior of two Ising spin models in 2D have been investigated by means of a sophisticated entropic

scheme based on the Wang–Landau algorithm. For the random bond square SAF model we have extracted accurate estimates for all critical exponents and two values of the disorder strength. These values verify hyperscaling, satisfy the Chayes *et al* inequality [8], and obey very well the weak universality scenario for disordered systems [112]. Furthermore, the strong saturating behavior of the specific heat clearly distinguishes this case of competing interactions from other 2D random bond systems studied previously. For the marginal case of the random bond Ising model, our findings favor the well-known double-logarithmic scaling scenario and suggest that the pure system behavior,  $\nu = 1$ , is recovered in the asymptotic limit. Here, the estimated critical temperatures, in both cases of disorder, are in excellent agreement with the exact values obtained by duality, reflecting the accuracy of the implemented entropic scheme. Encouraged by this latter observation, we are currently carrying out a similar study of bond disorder effects in 2D systems undergoing first-order phase transitions.

## Acknowledgments

We thank V Martín-Mayor and W Selke for useful e-mail correspondence. This research was supported by the Special Account for Research Grants of the University of Athens under Grant Nos 70/4/4071 and 70/4/4096. N G Fytas acknowledges financial support by the Alexander S Onassis Public Benefit Foundation.

## References

- [1] Imry Y and Wortis M, 1979 *Phys. Rev. B* **19** 3580
- [2] Aizenman M and Wehr J, 1989 *Phys. Rev. Lett.* **62** 2503  
Aizenman M and Wehr J, 1990 *Phys. Rev. Lett.* **64** 1311 (erratum)
- [3] Hui K and Berker A N, 1989 *Phys. Rev. Lett.* **62** 2507  
Hui K and Berker A N, 1989 *Phys. Rev. Lett.* **63** 2433 (erratum)  
Berker A N, 1990 *Phys. Rev. B* **42** 8640
- [4] Chen S, Ferrenberg A M and Landau D P, 1995 *Phys. Rev. E* **52** 1377
- [5] Chatelain C, Berche B, Janke W and Berche P E, 2001 *Phys. Rev. E* **64** 036120
- [6] Fernández L A, Gordillo-Guerrero A, Martín-Mayor V and Ruiz-Lorenzo J J, 2008 *Phys. Rev. Lett.* **100** 057201
- [7] Harris A B, 1974 *J. Phys. C: Solid State Phys.* **7** 1671
- [8] Chayes J T, Chayes L, Fisher D S and Spencer T, 1986 *Phys. Rev. Lett.* **57** 2999
- [9] Dotsenko V, Picco M and Pujol P, 1995 *Nucl. Phys. B* **455** 701
- [10] Cardy J, 1996 *J. Phys. A: Math. Gen.* **29** 1897
- [11] Jacobsen J L and Cardy J, 1998 *Nucl. Phys. B* **515** 701
- [12] Olson T and Young A P, 2000 *Phys. Rev. B* **61** 12467
- [13] Chatelain C and Berche B, 2000 *Nucl. Phys. B* **572** 626
- [14] Mazzeo G and Kühn R, 1999 *Phys. Rev. E* **60** 3823
- [15] Fytas N G, Malakis A and Eftaxias K, 2008 *J. Stat. Mech.* P03015
- [16] Fytas N G, Malakis A and Georgiou I, 2008 *J. Stat. Mech.* L07001
- [17] Butera P and Pernici N, 2008 *Phys. Rev. B* **78** 054405
- [18] Dotsenko V S and Dotsenko V S, 1981 *Sov. Phys. JETP Lett.* **33** 37  
Dotsenko V S and Dotsenko V S, 1983 *Adv. Phys.* **32** 129
- [19] Shalaev B N, 1984 *Sov. Phys.—Solid State* **26** 1811
- [20] Cardy J L, 1986 *J. Phys. A: Math. Gen.* **19** L193
- [21] Shankar R, 1987 *Phys. Rev. Lett.* **58** 2466  
Ludwig A W W, 1988 *Phys. Rev. Lett.* **61** 2388  
Ceccatto H A and Naon C, 1988 *Phys. Rev. Lett.* **61** 2389
- [22] Ludwig A W W, 1987 *Nucl. Phys. B* **285** 97
- [23] Ludwig A W W and Cardy J L, 1987 *Nucl. Phys. B* **285** 687
- [24] Mayer I O, 1989 *J. Phys. A: Math. Gen.* **22** 2815

- [25] Wang J-S, Selke W, Dotsenko V S and Andreichenko V B, 1990 *Physica A* **164** 221
- [26] Ludwig A W W, 1990 *Nucl. Phys. B* **330** 639
- [27] Ziegler K, 1990 *Nucl. Phys. B* **344** 499
- [28] Wang J-S, Selke W, Dotsenko V S and Andreichenko V B, 1990 *Europhys. Lett.* **11** 301
- [29] Heuer H, 1992 *Phys. Rev. B* **45** 5691
- [30] Shalaev B N, 1994 *Phys. Rep.* **237** 129
- [31] Kim J-K and Patrascioiu A, 1994 *Phys. Rev. Lett.* **72** 2785
- Kim J-K and Patrascioiu A, 1994 *Phys. Rev. B* **49** 15764
- Selke W, 1994 *Phys. Rev. Lett.* **73** 3487
- Ziegler K, 1994 *Phys. Rev. Lett.* **73** 3488
- Kim J-K and Patrascioiu A, 1994 *Phys. Rev. Lett.* **73** 3489
- Kim J-K, 2000 *Phys. Rev. B* **61** 1246
- [32] Kühn R, 1994 *Phys. Rev. Lett.* **73** 2268
- [33] de Queiroz S L A and Stinchcombe R B, 1994 *Phys. Rev. B* **50** 9976
- [34] Talapov A L and Shchur L N, 1994 *Europhys. Lett.* **27** 193
- Talapov A L and Shchur L N, 1994 *J. Phys.: Condens. Matter* **6** 8295
- [35] Mussardo G and Simonetti P, 1995 *Phys. Lett. B* **351** 515
- [36] Araújo Reis F D A, de Queiroz S L A and dos Santos R R, 1996 *Phys. Rev. B* **54** R9616
- [37] Jug G and Shalaev B N, 1996 *Phys. Rev. B* **54** 3442
- [38] Cabra D C, Honecker A, Mussardo G and Pujol P, 1997 *J. Phys. A: Math. Gen.* **30** 8415
- [39] Ballesteros H G, Fernández L A, Martín-Mayor V, Muñoz Sudupe A, Parisi G and Ruiz-Lorenzo J J, 1997 *J. Phys. A: Math. Gen.* **30** 8379
- [40] Araújo Reis F D A, de Queiroz S L A and dos Santos R R, 1997 *Phys. Rev. B* **56** 6013
- [41] Selke W, Szalma F, Lajko P and Igloi F, 1997 *J. Stat. Phys.* **89** 1079
- [42] Roder A, Adler J and Janke W, 1998 *Phys. Rev. Lett.* **80** 4697
- Roder A, Adler J and Janke W, 1999 *Physica A* **265** 28
- [43] Selke W, Shchur L N and Vasilyev O A, 1998 *Physica A* **259** 388
- [44] Araújo Reis F D A, de Queiroz S L A and dos Santos R R, 1999 *Phys. Rev. B* **60** 6740
- [45] Luo H J, Schülke L and Zheng B, 2001 *Phys. Rev. E* **64** 036123
- [46] Nobre F D, 2001 *Phys. Rev. E* **64** 046108
- [47] Shchur L N and Vasilyev O A, 2001 *Phys. Rev. E* **65** 016107
- [48] Tomita Y and Okabe Y, 2001 *Phys. Rev. E* **64** 036114
- [49] Merz F and Chalker J T, 2002 *Phys. Rev. B* **65** 054425
- [50] Calabrese P, Orlov E V, Pakhnin V and Sokolov A I, 2004 *Phys. Rev. B* **70** 094425
- [51] de Queiroz S L A, 2006 *Phys. Rev. B* **73** 064410
- [52] Lessa J C and de Queiroz S L A, 2006 *Phys. Rev. E* **74** 021114
- [53] Picco M, Honecker A and Pujol P, 2006 *J. Stat. Mech.* P09006
- [54] Kenna R, Johnston D A and Janke W, 2006 *Phys. Rev. Lett.* **96** 115701
- Kenna R, Johnston D A and Janke W, 2006 *Phys. Rev. Lett.* **97** 155702
- [55] Martins P H L and Plascak J A, 2007 *Phys. Rev. E* **76** 012102
- [56] Hasenbusch M, Toldin F P, Pelissetto A and Vicari E, 2008 *Phys. Rev. E* **78** 011110
- [57] Hadjiagapiou I A, Malakis A and Martinos S S, 2008 *Physica A* **387** 2256
- [58] Kenna R and Ruiz-Lorenzo J J, 2008 *Phys. Rev. E* **78** 031134
- [59] Suzuki M, 1974 *Prog. Theor. Phys.* **51** 1992
- [60] Gunton J D and Niemeijer T, 1975 *Phys. Rev. B* **11** 567
- [61] Wang F and Landau D P, 2001 *Phys. Rev. Lett.* **86** 2050
- Wang F and Landau D P, 2001 *Phys. Rev. E* **64** 056101
- [62] Malakis A, Peratzakis A and Fytas N G, 2004 *Phys. Rev. E* **70** 066128
- Malakis A, Martinos S S, Hadjiagapiou I A, Fytas N G and Kalozoumis P, 2005 *Phys. Rev. E* **72** 066120
- [63] Belardinelli R E and Pereyra V D, 2007 *Phys. Rev. E* **75** 046701
- Belardinelli R E and Pereyra V D, 2007 *J. Chem. Phys.* **127** 184105
- [64] Metropolis N, Rosenbluth A W, Rosenbluth M N and Teller A H, 1953 *J. Chem. Phys.* **21** 1087
- [65] Bortz A B, Kalos M H and Lebowitz J L, 1975 *J. Comput. Phys.* **17** 10
- [66] Binder K, 1997 *Rep. Prog. Phys.* **60** 487
- [67] Newman M E J and Barkema G T, 1999 *Monte Carlo Methods in Statistical Physics* (Oxford: Clarendon)
- [68] Landau D P and Binder K, 2000 *A Guide to Monte Carlo Simulations in Statistical Physics* (Cambridge: Cambridge University Press)
- [69] Lee J, 1993 *Phys. Rev. Lett.* **71** 211

- [70] Lee H K, Okabe Y and Landau D P, 2006 *Comput. Phys. Commun.* **175** 36
- [71] de Oliveira P M C, Penna T J P and Herrmann H J, 1996 *Braz. J. Phys.* **26** 677
- [72] Wang J-S, Tay T K and Swendsen R H, 1999 *Phys. Rev. Lett.* **82** 476  
Wang J-S and Swendsen R H, 2002 *J. Stat. Phys.* **106** 245
- [73] Berg B A and Neuhaus T, 1991 *Phys. Lett. B* **276** 249  
Berg B A and Neuhaus T, 1992 *Phys. Rev. Lett.* **68** 9
- [74] Smith G R and Bruce A D, 1995 *J. Phys. A: Math. Gen.* **28** 6623
- [75] Torrie G M and Valleau J-P, 1997 *J. Comput. Phys.* **23** 187
- [76] Swendsen R H and Wang J-S, 1986 *Phys. Rev. Lett.* **57** 2607
- [77] Geyer C J, 1991 *Computing Science and Statistics: Proc. 23rd Symp. on the Interface* ed E K Keramidas (New York: Interface Foundation, Fairfax Station) p 156
- [78] Marinari E and Parisi G, 1992 *Europhys. Lett.* **19** 451
- [79] Lyubartsev A P, Martsinovskii A A, Shevkunov S V and Vorontsov-Velyaminov P N, 1992 *J. Chem. Phys.* **96** 1776
- [80] Hukushima K and Nemoto K, 1996 *J. Phys. Soc. Japan* **65** 1604
- [81] Marinari E, Parisi G and Ruiz-Lorenzo J, 1998 *Spin Glasses and Random Fields (Directions in Condensed Matter Physics vol 12)* ed A P Young (Singapore: World Scientific)
- [82] Trebst S, Huse D A and Troyer M, 2004 *Phys. Rev. E* **70** 046701
- [83] Douarche N, Calvo F, Pastor G M and Jensen P J, 2003 *Eur. Phys. J. D* **24** 77
- [84] Troyer M, Wessel S and Alet F, 2003 *Phys. Rev. Lett.* **90** 120201
- [85] Malakis A and Fytas N G, 2006 *Phys. Rev. E* **73** 056114  
Malakis A and Fytas N G, 2006 *Phys. Rev. E* **73** 016109  
Malakis A and Fytas N G, 2006 *Eur. Phys. J. B* **51** 257  
Malakis A, Fytas N G and Kalozoumis P, 2007 *Physica A* **383** 351  
Fytas N G and Malakis A, 2008 *Eur. Phys. J. B* **61** 111
- [86] Schulz B J, Binder K and Müller M, 2005 *Phys. Rev. E* **71** 046705
- [87] Reynal S and Diep H T, 2005 *Phys. Rev. E* **72** 056710
- [88] Jayasri D, Sastry V S S and Murthy K P N, 2005 *Phys. Rev. E* **72** 036702
- [89] Trebst S, Gull E and Troyer M, 2005 *J. Chem. Phys.* **123** 204501
- [90] Rathore N and de Pablo J J, 2002 *J. Chem. Phys.* **116** 7225  
Rathore N, Knotts T A and de Pablo J J, 2003 *J. Chem. Phys.* **118** 4285  
Rathore N, Yan G and de Pablo J J, 2004 *J. Chem. Phys.* **120** 5781  
Yan Q, Faller R and de Pablo J J, 2002 *J. Chem. Phys.* **116** 8745
- [91] Shell M S, Debenedetti P G and Panagiotopoulos A Z, 2002 *Phys. Rev. E* **66** 056703
- [92] Yamaguchi C and Okabe Y, 2001 *J. Phys. A: Math. Gen.* **34** 8781  
Okabe Y, Tomita Y and Yamaguchi C, 2002 *Comput. Phys. Commun.* **146** 63
- [93] Varshney V and Carri G A, 2005 *Phys. Rev. Lett.* **95** 168304  
Carri G A, Batman R, Varshney V and Dirama T E, 2006 *Polymer* **46** 3809
- [94] Calvo F, 2002 *Mol. Phys.* **100** 3421  
Calvo F and Parneix P, 2003 *J. Chem. Phys.* **119** 256
- [95] Tsai S-H, Wang F and Landau D P, 2007 *Phys. Rev. E* **75** 061108  
Tsai S-H, Wang F and Landau D P, 2008 *Braz. J. Phys.* **38** 6  
Seaton D T, Mitchell S J and Landau D P, 2008 *Braz. J. Phys.* **38** 48  
Mitchell S J, Luiz Pereira F C and Landau D P, 2008 *Braz. J. Phys.* **38** 1
- [96] Vorontsov-Velyaminov P N, Volkov N A and Yurchenko A A, 2004 *J. Phys. A: Math. Gen.* **37** 1573  
Volkov N A, Vorontsov-Velyaminov P N and Lyubartsev A P, 2007 *Phys. Rev. E* **75** 016705
- [97] Poulain P, Calvo F, Antoine R, Broyer M and Dugourd P, 2006 *Phys. Rev. E* **73** 056704
- [98] Schulz B J, Binder K, Müller M and Landau D P, 2003 *Phys. Rev. E* **67** 067102
- [99] Dayal P, Trebst S, Wessel S, Würtz D, Troyer M, Sabhapandit S and Coppersmith S N, 2004 *Phys. Rev. Lett.* **92** 097201
- [100] Alder S, Trebst S, Hartmann A K and Troyer M, 2004 *J. Stat. Mech.* **P07008**
- [101] Zhou C and Bhatt R N, 2005 *Phys. Rev. E* **72** 025701(R)  
Zhou C, Schulthess T C, Torbrügge S and Landau D P, 2006 *Phys. Rev. Lett.* **96** 120201
- [102] Swendsen R H and Krinsky S, 1979 *Phys. Rev. Lett.* **43** 177
- [103] Binder K and Landau D P, 1980 *Phys. Rev. B* **21** 1941
- [104] Oitmaa J and Velgakis M J, 1987 *J. Phys. A: Math. Gen.* **20** 1269
- [105] Landau D P and Binder K, 1985 *Phys. Rev. B* **31** 5946
- [106] Tanaka K, Horiguchi T and Morita T, 1992 *Phys. Lett. A* **165** 266

- [107] Minami K and Suzuki M, 1994 *J. Phys. A: Math. Gen.* **27** 7301
- [108] Malakis A, Kalozoumis P and Tyraskis N, 2006 *Eur. Phys. J. B* **50** 63
- [109] Wu F Y, 1982 *Rev. Mod. Phys.* **54** 235
- [110] Monroe J L and Kim S I, 2007 *Phys. Rev. E* **76** 021123
- [111] Ferrenberg A M and Landau D P, 1991 *Phys. Rev. B* **44** 5081
- [112] Kim J-K, 1996 *Phys. Rev. B* **53** 3388
- [113] Holm C and Janke W, 1994 *J. Phys. A: Math. Gen.* **27** 2553
- [114] Picco M, 1996 *Phys. Rev. B* **96** 14930
- [115] Fisch R, 1978 *J. Stat. Phys.* **18** 111
- [116] Kinzel W and Domany E, 1981 *Phys. Rev. B* **23** 3421